Quantitative Imaging of Flow through a Mechanical Heart Valve

Peter Oshkai*, Juan Mejia†, and Brett Wootton‡
University of Victoria, Victoria, BC, V8W 3P6, Canada

Vortex formation due to turbulent inflow through a bileaflet prosthetic heart valve is investigated using a technique of digital particle image velocimetry. The emphasis is on the natural vortex shedding from the valve leaflets. Classes of vortex formation are characterized in terms of global instantaneous and time-averaged patterns of velocity, vorticity, and streamline topology. This image-based approach provides an insight into the underlying flow physics, including the interaction between shear layers that form downstream of the valve.

Nomenclature

$\underline{V}$	=	Instantaneous flow velocity
ω_z	=	Out-of-plane vorticity
u_{rms}	=	Root mean square of the streamwise velocity component.
v_{rms}	=	Root mean square of the transverse velocity component.
$\langle\underline{V}\rangle$	=	Time-averaged flow velocity
$\langle\omega_z\rangle$	=	Time-averaged vorticity
$\langle u'v'\rangle$	=	Time averaged Reynolds stress correlation

I. Introduction

The human heart is a pump, with four chambers and four valves, which circulates blood in the body. It pumps about 5.25 liters of blood per minute and on average beats about 2.5 billion times in a lifetime. Among the most common types of heart diseases are heart valve failures, with the most commonly affected valves being the aortic, mitral, and tricuspid valves. Consequently, implanting prosthetic heart valves, either mechanical or biological ones, has been used as a surgical treatment for heart valve disease.

The first heart valve was implanted in 1952. Since then, mechanical heart valves (MHVs) of various types, such as caged ball, tilting disk, bileaflet, trileaflet, as well as various biological valves have been developed.

There are number of problems associated with prosthetic heart valves. The complications directly associated with fluid dynamics are[1, 2]:

a) thromboembolism,
b) tissue overgrowth,
c) blood cell damage,
d) damage of the tissue adjacent to the valve,
e) valve failure due to material fatigue or chemical change,
f) large pressure gradients across the valve.

Relative advantages and disadvantages of mechanical and biological heart valves can be summarized as follows: Mechanical Heart Valves (MHVs) are relatively durable but are strongly associated with thromboembolisms, which often result in ischemic attacks and stroke[3]. Thrombi are believed to be caused by flow phenomena that are not characteristic of physiological conditions[4]. The flow phenomena that receive the most attention in this respect are: jet-like flow regions, regions of elevated shear stresses, flow separation regions, shed vortices, and turbulence

* Assistant Professor, Department of Mechanical Engineering, University of Victoria, PO Box 3055 STN CSC Victoria, BC, Canada V8W 3P6.
† Research Assistant, Department of Mechanical Engineering, University of Victoria.
‡ Research Assistant, Department of Mechanical Engineering, University of Victoria.

characteristics[3]. Despite the recent advances in the field, thromboembolism occurs in approximately 3% of all replacement operations involving MHVs[5].

On the other hand, biological valves exhibit relatively large pressure drops, deteriorate faster, and undergo rapid calcification[1, 2]. However, biological prosthetic heart valves do not require the use of blood thinners by the patient, making them an attractive alternative to MHVs.

A number of experimental and numerical studies have been undertaken in order to address problems with both biological and mechanical heart valves. Although there have been several advances in the field, the fundamental governing fluid phenomena are still not adequately understood.

A. Experimental studies

Significant effort has been devoted over the years to developing realistic laboratory models capable of simulating fluid mechanic characteristics of the human heart while allowing optical access for the purposes of flow visualization. The complexity of the biological system calls for a compliant setup that not only preserves geometric similarity but also models the pumping cycle. Anatomically correct mock-ups of the aorta have been successfully manufactured and investigated. Yip *et al.* [6] were the first to fabricate a compliant model that included aortic sinuses, ascending aorta, and aortic arch. Scotten *et al.*[7] developed a compliant model of the left heart, which allowed the simulation of an arbitrary cardiac cycle and provided optical access to valves in both the aortic and the mitral positions. Several studies have been conducted with this setup, including the development of a new technique to measure the projected dynamic area of prosthetic heart valves[7].

It has been suggested that among the many possible causes of thromboembolism, vortex shedding from the leaflets of MHVs is one of the most critical. The shed vortices are associated with regions of high shear stress in the flow. Blood cells, e.g. activated platelets, can become entrapped within the shed vortices for relatively long periods of time, thus increasing the chance of thrombus formation.

Bluestein *et al.*[8] performed a study of a pulsatile flow through a bileaflet MHV mounted in a non-compliant aorta model. A technique of digital particle image velocimetry (DPIV) was used to characterize the flow. The authors assumed (based on the results of Lamson *et al.*[9]) that no single phase of the heart cycle (i.e. opening, fully open, closure, and fully closed) contributes significantly more to the formation of thrombi compared to the other phases. However, a number of other investigations focused on a particular phase of the cardiac cycle. In fact, during the 1970's and 1980's, most of the studies implicitly assumed that blood damage occurs predominantly during forward peak flow trough the valve. This assumption is intuitive, as the flow rate is at its maximum when the valve is fully open. At present, there is no clear consensus in the research community on whether a certain phase of the cardiac cycle contributes the most to blood cell damage.

Several studies focused on the fundamental fluid dynamics of MHVs in order to provide insight into the flow phenomena. Castellini *et al.*[10] employed particle image velocimetry (PIV) techniques to obtain flow velocity measurements upstream and downstream of a bileaflet valve. A symmetric flow pattern including a large separation region behind each leaflet was observed. Furthermore, the authors observed regions of high velocity between the leaflets as well as between each leaflet and the channel walls, which represented the walls of the aorta. Vortex shedding from the trailing edge of each leaflet was also documented. Zhao *et al.*[11] investigated the flow fields corresponding to different valve positions. The flow patterns were found to be symmetric, with separation regions present on the inner surface of the leaflets. The pulsatile flow was modeled by employing a pressure waveform corresponding to a typical cardiac cycle. In order to compensate for the limited temporal resolution of the PIV measurements, the waveform was stretched over a period of 10 seconds.

B. Numerical studies

Computational methods, in comparison to experiments, have the advantage of not being limited by physical boundaries. For example, with PIV, it is necessary to have an optical path between the camera and the flow field that is free of distortions. In addition, numerical simulations can provide detailed three-dimensional, time-resolved information about the flow. Hence, an integrated approach involving both experimental and numerical techniques is often required to fully characterize a fluid flow problem.

Since platelet activation is closely linked to occurrence of thromboembolisms, a number of studies focused on the effect of prosthetic heart valves on platelet activation. A platelet is considered to be active if it reached a certain threshold of cumulative exposure to high shear stress. The platelet activation state (PAS) was studied for monoleaflet and bileaftlet valves by Yin *et al.*[3] The authors considered both shear stress magnitude and time of exposure of a given platelet to the elevated shear stress to determine the PAS. In order to determine the amount of activated platelets numerically, tracers were introduced to the calculated flow. The exposure of a tracer to shear stresses over a period of time was then evaluated. Monoleaflet valves were found to cause less PAS compared to

bileaflet valves. Furthermore, the results showed that virtually no PAS existed in a control case when the valve was removed from the flow field.

A numerical simulation of the closing phase of a bileaflet MHV was performed by Lai *et al.*[12] It was found that the negative pressure quickly develops on the atrial side of a valve leaflet tip and on the valve housing. The pressure reaches its lowest value just before the valve fully closes. It was determined that the low local pressure is caused by the dynamics of the shed vortices. Furthermore, it was shown that the clearance gap and tip angle of the valve does not influence the associated fluid dynamics significantly. On the other hand, the speed at which the leaflet closes can have a dramatic effect in terms of the local pressure decrease. In fact, the study showed that reducing the velocity in the last four degrees of the motion by a factor of three leads to a reduction of both the maximum positive and negative pressures by more than 50%. This numerical simulation did not take into account coupling between the wakes caused by the two leaflets that was observed by Hirt *et al.*[13]

II. Experimental System and Techniques

C. Testing facility

The present experiments were performed using water as a working fluid. The complete flow facility, illustrated in Fig.1, consisted of a Plexiglas duct, the test section, flexible tubing, water reservoir, and a centrifugal pump. A prosthetic heart valve (PHV) chamber was designed to provide distortion-free optical access to the region downstream of the heart valve. The water was supplied by a 2HP centrifugal pump, and the flow rate was adjusted by a valve system.

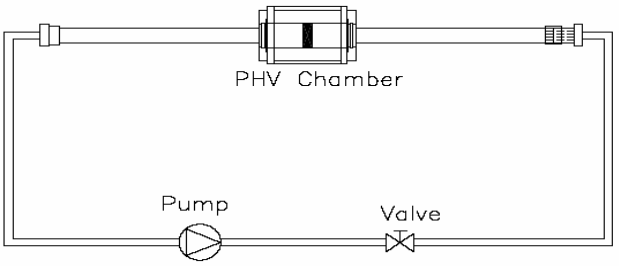

Figure 1. Schematic of flow facility

The test section was located 254 mm downstream of the main duct inlet. A honeycomb flow straightener was deployed directly downstream of the inlet. In order to minimize optical distortions, the test section was surrounded by a prismatic acrylic chamber filled with distilled water. A bileaflet mechanical heart valve was mounted in a straight circular channel 20.39 mm in diameter. A unidirectional flow was maintained at approximately 0.35 m/s. A detailed schematic of the test section is provided in Fig. 2.

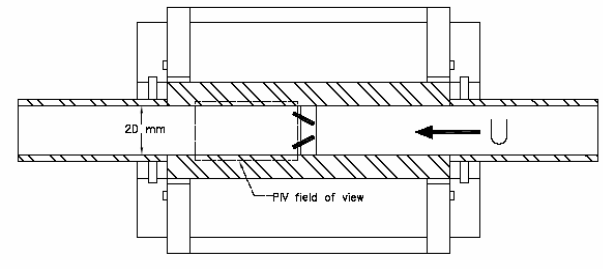

Figure 2. Schematic of test section

D. Techniques of particle image velocimetry

Quantitative flow visualization was accomplished by employing a digital version of particle image velocimetry (DPIV). The water flow was seeded with glass spheres with the typical diameter of approximately 10 μm, which served as tracer particles for the flow. Images of the particles, which were illuminated by a laser, were captured by a high-resolution digital camera. These images were then processed on a computer to yield the instantaneous flow velocity measurements, vorticity, as well as time-averaged flow parameters. The displacement of the particles was recorded as a pair of images each exposed once. The recorded particle displacement field was measured locally across the whole field of view of the images, scaled by the image magnification and then divided by the known laser pulse separation to obtain flow velocity at each point. The CCD camera was positioned perpendicular to the plane of the light. Depending on the flow velocity and the factor of magnification of the camera lens, the delay of the two pulses was chosen such that adequate displacements of the particle images on the CCD were obtained. From the time delay between the two illuminations and the displacement of the tracers, velocity vectors were be calculated.

For the present study, a lens with a focal length of 60 mm was used in conjunction with a 1376 x 1040 pixel CCD to provide a physical resolution of the velocity vector field of 4 vectors per square millimeter.

The PIV images were acquired at a time interval of 0.204 s, which provided spacing in time appropriate for obtaining random samples for the calculation of averaged turbulence statistics. A total of 300 images were acquired and used in the calculation of the following time-averaged parameters: flow velocity $\langle \underline{V} \rangle$ (not presented here), out-of-plane vorticity $\langle \omega_z \rangle$, root-mean-square values of velocity components $\langle u_{rms} \rangle$ and $\langle v_{rms} \rangle$, and Reynolds stress correlation $\langle u'v' \rangle$.

III. Flow Structure Downstream of a Bileaflet Mechanical Heart Valve

Rosenfeld *et al.*[14] identified the following basic sources of flow unsteadiness for the case of mechanical heart valve:

a) Natural vortex shedding;

b) Time variations due to unsteady inflow;

c) Motion of the valve.

The emphasis of the present study is on the natural vortex shedding from the valve leaflets. Previously, the vortex shedding frequency was estimated to be of the order of 25 Hz for the case of monoleaflet valve and an inflow velocity of 60 cm/sec.[15] Therefore, several vortex shedding cycles can take place during the fully-open phase of the valve motion cycle. The present investigation focuses on the flow through a fully-open bileaflet valve, which is mounted in a circular channel and is subjected to a unidirectional turbulent inflow.

E. Instantaneous Flow Patterns

Patterns of instantaneous flow velocity $\underline{V}$ and corresponding out-of-plane vorticity ω_z in the wake of a bileaflet valve are shown in Figs. 3 through 5. The images are obtained at the plane of symmetry of the channel (Fig. 2) and correspond to a Reynolds number of 9500. The leaflets of the fully-open valve are indicated by the gray shaded areas. The regions between the leaflets as well as directly below the lower leaflet do not show velocity vectors due to optical inaccessibility. A unidirectional turbulent inflow is directed from right to left.

Generally, the following flow structure is observed downstream of the valve:

Shear layers are formed at the tips of both leaflets. The outer shear layers, which form at the trailing edges of the leaflets, roll up into vortices that are shed. It is traditionally assumed that the inner shear layers, which form at the leading edges, roll into vortices that stay attached to the leaflet surface. There is evidence from previous investigations[13] that the inner vortices can also be shed if the valve motion is considered. However, the authors reported that the vortices shed from the outer edges of the leaflets remain dominant during all phases of the valve motion. Present observations indicate that for the case of unidirectional flow through a fully-open valve, vortex shedding occurs from both the inner and outer tips of the leaflets. Moreover, a relatively low-frequency, large-scale flow oscillation was observed in addition to the vortex shedding from the tips of the leaflets. Figures 3 through 5 illustrate three characteristic phases of this oscillation. These phases are referred to as dominant lower wake regime (Fig. 3), symmetric wake regime (Fig. 4), and dominant upper wake regime (Fig. 5).

Figure 3 corresponds to a time instant when the wake from the lower leaflet dominates the flow field. The velocity vector plot of Fig. 3(a) shows that the low velocity region corresponding to the lower wake occupies a significantly larger area compared to the upper wake. In addition, the velocity plot shows a pronounced upward deflection of the jet-like flow that exists between the valve leaflets.

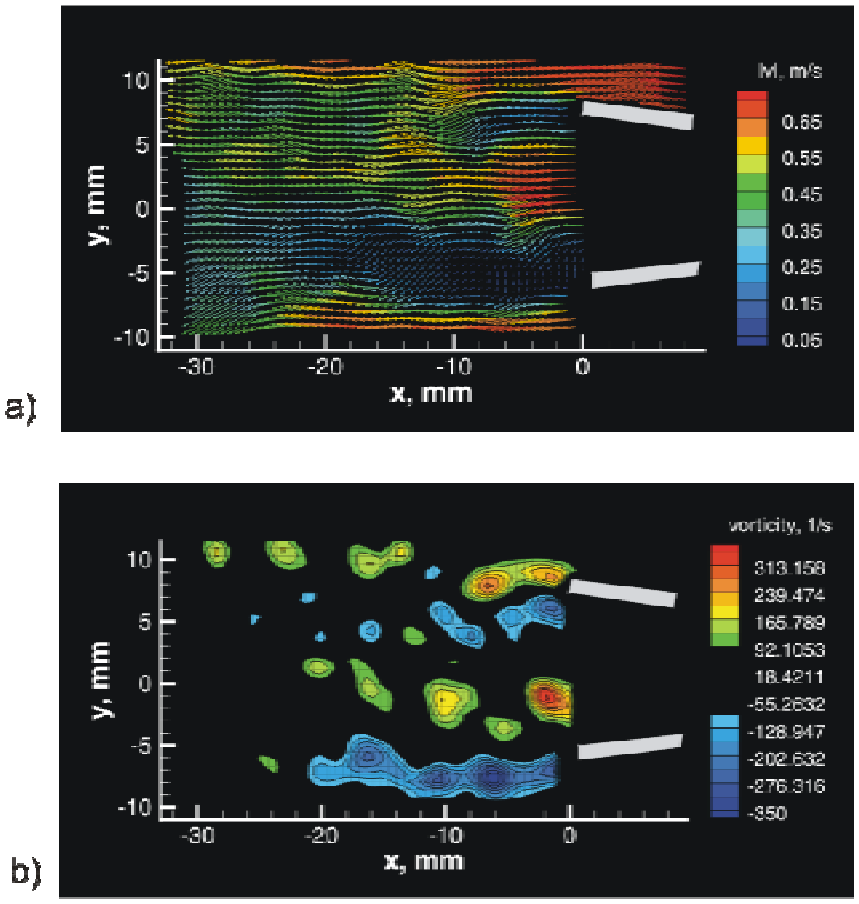

Figure 3. Instantaneous patterns of velocity (a) and out-of-plane vorticity (b). Dominant lower wake regime.

The wake of the lower leaflet exhibits significantly higher levels of vorticity, compared to the upper wake. The vorticity contour plot of Fig. 3(b) shows that the outer shear layer of the bottom leaflet contains three well-defined negative vortices that were shed from the trailing edge of the leaflet. The inner shear layer of the lower leaflet also contains shed vortices. The distance between these positive vortices indicates that their shedding frequency is similar to that of the vortices in the outer shear layer. Moreover, the vortices in the outer and inner shear layers of the lower leaflet retain substantial levels of circulation up to 20 mm downstream of the valve.

In contrast to the lower leaflet, the outer and inner shear layers of the upper leaflet are located significantly closer to each other. In particular, the negative vortices of the inner layer develop close to the leaflet surface and interact with the positive vortices of the outer shear layer by forming counter-rotating vortex pairs. This interaction between the counter-rotating vortices results in a rapid decrease of their circulation levels with the downstream distance. Rapid dissipation of vorticity due to shear layer interaction results in the early collapse of the upper wake, which extends only 10 mm downstream of the valve. This collapse is accompanied by the upward deflection of the inner shear layer of the lower leaflet.

The next characteristic phase of the flow oscillation cycle is referred to as symmetric wake regime and is illustrated in Fig. 4. During this phase, the four shear layers do not exhibit large-scale transverse deflections. Shed vortices of the inner shear layers form counter-rotating vortex pairs. The shear layers retain substantial vorticity levels up to approximately 15 mm downstream of the valve. The symmetric wake regime constitutes a transition between the dominant lower wake phase of Fig. 3 and the dominant upper wake phase, which is illustrated in Fig. 5.

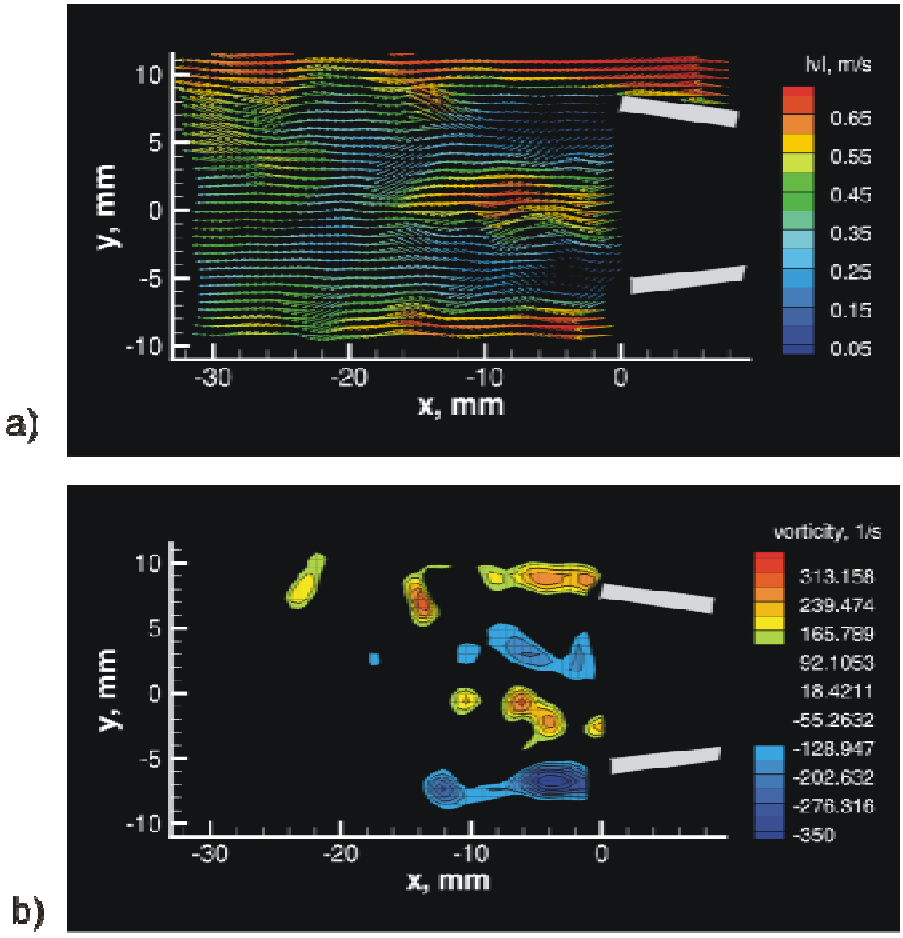

Figure 4. Instantaneous patterns of velocity (a) and out-of-plane vorticity (b). Symmetric wake regime.

Patterns of instantaneous flow velocity and out-of-plane vorticity shown in Fig. 5 correspond to the flow oscillation phase which is opposite to the dominant lower wake regime of Fig. 3. Figure 5(a) shows that the lower velocity region that forms behind the upper leaflet dominates the flow field. Rapid dissipation of positive vorticity in the inner shear layer of the lower leaflet is accompanied by a large-scale downward deflection of the inner shear layer of the upper leaflet and the associated jet-like flow in the middle of the channel.

It is evident that the frequency of the large-scale flow oscillation that is represented by the sequence of images in Figs. 3 through 5 is substantially lower than the frequency of the vortex shedding from the tips of the leaflets. In fact, at least four small-scale vortices are shed from the leaflet tips during each of the characteristic phases of the large-scale oscillation cycle described above. Limited temporal resolution of the DPIV imaging sequence did not allow accurate estimation of the large-scale oscillation frequency. The large-scale flow oscillation corresponds to transverse undulations of the jet-like flow through the central opening of the valve and to flapping of the associated inner shear layers.

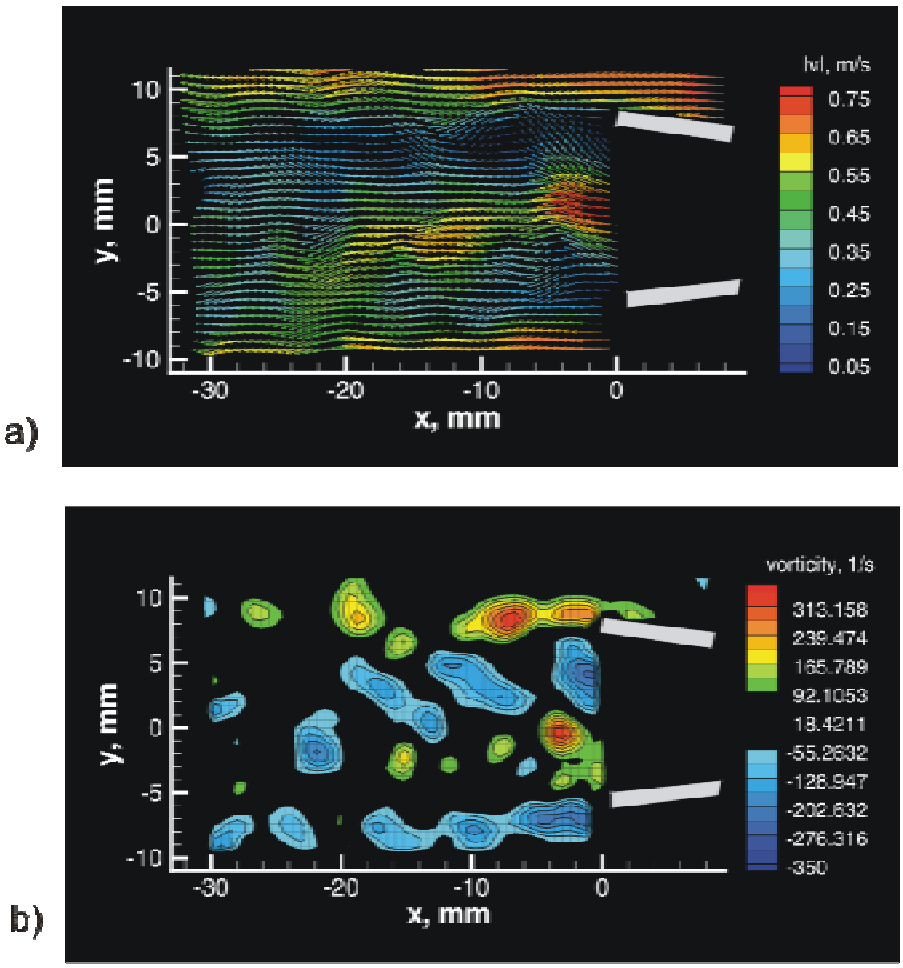

Figure 5. Instantaneous patterns of velocity (a) and out-of-plane vorticity (b). Dominant upper wake regime.

F. Time-averaged Flow Patterns

The general structure of the wake downstream of the bileaflet heart valve is clearly evident in the plot of time-averaged vorticity $\langle\omega_z\rangle$, which is shown in Fig. 6. This plot was obtained by ensemble-averaging 300 instantaneous images, similar to those presented in the previous section. The dominant feature of the flow field downstream of the valve is the presence of four separated shear layers that form at the tips of the leaflets. The outer shear layers form at the trailing edges of the upper and lower leaflet. They are indicated in Fig.5 by the regions of high positive and negative time-averaged vorticity respectively, which extend approximately 16 mm downstream of the valve. The inner shear layers, which form at the leading edges of the leaflets, exhibit high levels of time-averaged vorticity of the opposite sign, relative to the outer shear layers. Due to highly unsteady nature of the inner shear layers, the time-averaged vorticity associated with them decreases rather rapidly with the downstream distance. In fact, no significant levels of vorticity exist in the central region of the channel beyond approximately 5 mm downstream of the valve.

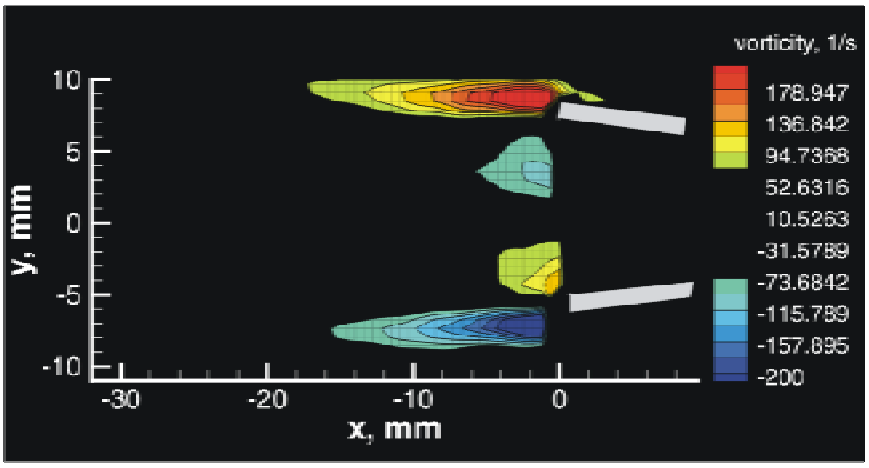

Figure 6. Time-averaged vorticity distribution.

Figures 7 and 8 show patterns of velocity fluctuations in the wake of the valve in terms of root-mean-square of horizontal and vertical velocity components respectively. High levels of u_{rms} are associated with the unsteadiness of the inner shear layers and the periodic growth and collapse of the wakes of the leaflets. The peak levels of u_{rms} of 0.2 m/s occur at the locations of the separation of the inner shear layers. Significant levels of u_{rms} are observed as far as 22 mm downstream of the valve.

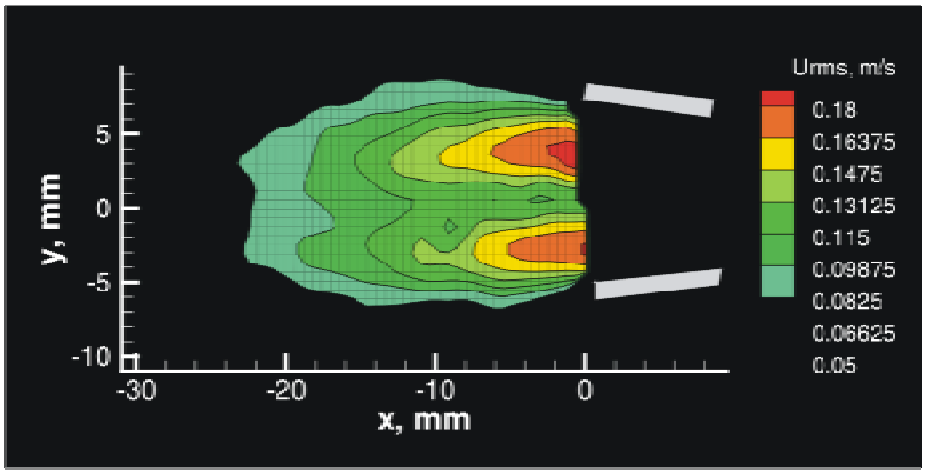

Figure 7. Root-mean-square of streamwise velocity fluctuations.

The peak values of v_{rms} of 0.12 m/s also occur at the location of the separation of the inner shear layers. Elevated values of v_{rms} are also associated with transverse undulations of the outer shear layers.

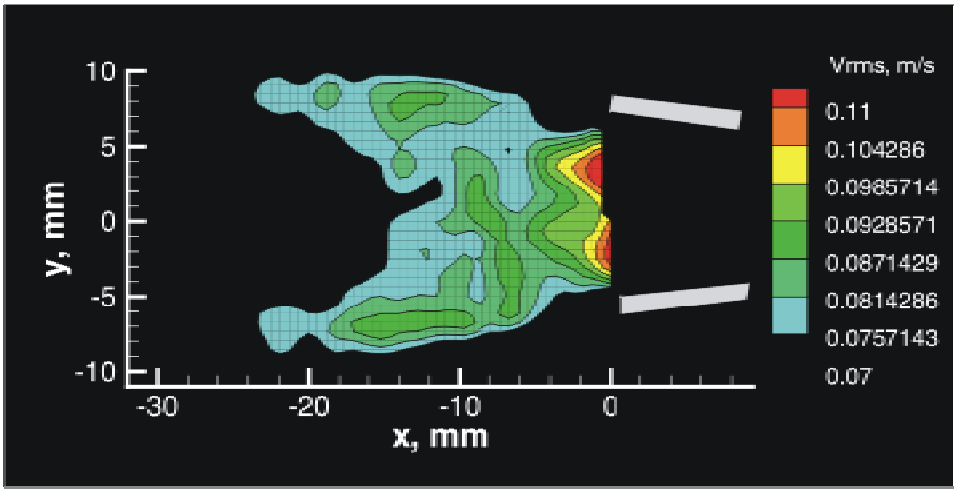

Figure 8. Root-mean-square of transverse velocity fluctuations.

The distribution of the velocity correlation <u′v′>, which corresponds to the dominant Reynolds shear stress component is shown in Fig. 9. Elevated values of <u′v′> are associated with the inner shear layers and the downstream sections of the outer shear layers. The peak values of ±0.01 m^2/s^2 occur in the near-wakes of the leaflets. Although limited temporal resolution of the DPIV imaging sequence did not allow the calculation of pathlines and hence the accurate evaluation of the platelet activation state (PAS), the plot of Fig. 9 provides an indication of the regions within the wake of the bileaflet valve that contribute the most to the platelet activation.

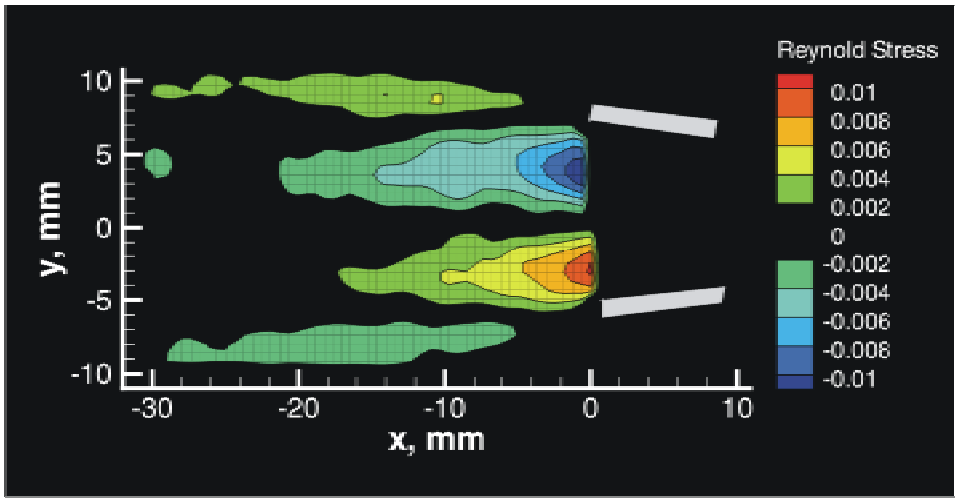

Figure 9. Reynolds stress correlation (<u′v′>).

IV. Concluding Remarks

Flow through mechanical heart valves (MHVs) has been a subject of extensive investigations over the years. Of particular interest is platelet activation, which is linked to occurrence of thromboembolisms. The present investigation is focused on the interactions between unsteady flow structures that occur due to natural vortex shedding from the valve leaflets. Analysis of instantaneous and time-averaged flow patterns in the wake of a fully-

open bileaflet heart valve under a unidirectional inflow conditions was performed using digital particle image velocimetry (DPIV). The general structure of the wake observed during this study is in agreement with previous investigations. The dominant features of the flow downstream of the valve are four separated shear layers that form at the leading and trailing edges of the two leaflets. Contrary to the traditional assumption of the dominant role of the outer shear layers, it was shown that the large-scale transverse oscillations of the inner shear layers dominate the near-wake of the valve. These oscillations were characterized in terms of three representative flow regimes. The dominant frequency of the large-scale flow instability is substantially lower than the frequency of the vortex shedding from the tips of the leaflets. Moreover, image-based analysis of the turbulence statistics provides insight into the plow physics associated with platelet activation. In particular, unsteady flow structures and mechanisms of their interactions most directly responsible for elevated shear stress in the flow field are identified and quantitatively assessed.

Acknowledgments

The authors would like to thank Dr. Ned Djilali of the University of Victoria for providing instrumentation for this study and for valuable comments. Moreover, the authors would like to thank Drs. Lawrence Scotten and David Walker of Vivitro Systems Inc. for extensive discussions.

The authors gratefully acknowledge financial support of Natural Sciences and Engineering Research Council of Canada (NSERC) under a Discovery Grant.

References

[1]Woo, Yi-Ren, Williams, F.P., Yoganathan, A.P., Nov. 1983, "In-Vitro Fluid Dynamic Characteristics of the Abiomed Trileaflet Heart Valve Prosthesis:", ASME, Vol. 105, 338-345.

[2]Yoganathan, A.P., He, Z., Jones, S. C., 2004, "Fluid Mechanics of Heart Valves", Annu. Rev. Biomed. Eng., Vol. 6, 331-362.

[3]Yin, W., Alemu, Y., Affeld, K., Jesty, J., Bluestien, D., August 2004, "Flow-Induced Platelet Activation in Bileaflet and Monoleaflet Mechanical Heart Valves", Annals of Bio. Eng., Vol. 32, No.8, 1058-1066.

[4]Bluestien, D., Yin, W., Affeld, K., and Jesty, J., 2004, "Flow- induced Platelet Activation in Mechanical Heart Valves", JHVD Vol. 13, 501-508.

[5]Edmunds, L. H., Mckinlay, S., Anderson, J. M., Callahan, T. H., Chesebro, J. H., Geiser, E. A., Makanani, D. M., McIntire, L. V., Meeker, W. Q., Naughton, G. N., Panza, J. A., Schoen, F. J., Didisheim, P., 1997, "Directions for improvement of substitute heart valves: National heart, lung and blood institute's working group report on heart valves", J. Biomed. Mater. Res., Vol 38, No. 3, 263-266.

[6]Yip, R., Mongrain, R., Ranga, A., Brunette, J., and Cartier, R., 2004, "Development of Anatomically Correct Mock-ups of the Aorta for PIV Investigations", Department of Mechanical Engineering, McGill University.

[7]Scotten, L. N., Walker, D. K., Jan. 2004, "New Laboratory Technique Measures Projected Dynamics Area of Prosthetic Heart Valves", J. Heart Valve Dis., Vol. 13, No. 1.

[8]Bluestein, D., Rambod, E., Gharib, M., April 2000, "Vortex Shedding as a Mechanism for Free Emboli Formation in Mechanical Heart Valves", J. of Bio. Eng., Vol. 122, 125-134.

[9]Lamson, T. C., Rosenberg, G., Geselowitz, D. B., Deutsch, S., Stinebring, D. R., Frangos, J. A., and Tarbell, J. M., 1993, "Relative Blood Damage in the Three Phases of a Prosthetic Heart Valve Flow Cycle", ASAIO J., Vol. 39, No. 3, M626-M633.

[10]Castellini, P., Marassi, M., Pinotti, P., Scalise, L., Tomasini, E. P., "Optical Measurement of Flow Properties in Artificial Heart Valves", Universita degli Studi di Ancona, Italy.

[11]Zhao, J. B., Yeo, J. H., "A Particle Image Volocimetry (PIV) study on the Pulsatile Flow Through Bileaflet Mechanical Aortic Heart Valves Under Physiological Conditions", School of Mechanical and Production Engineering, Nanyang Tech. University, Singapore.

[12]Lai, Y. G., Chandran, K. B., Lemmon, J., 2002, "A Numerical Simulation of Mechanical Heart Valve Closure Fluid Dynamics", J. of Biomechanics, Vol. 35, 881-892.

[13]Hirt, F., Iten, R., Ziada, S., 1997, "Flow-Induces Oscillations of a Butterfly-Valve: Prediction of the Frequency Behaviour", ASME, Vol 2, 499-505.

[14]Rosenfeld, M., Avrahami, I., Einav, S., 2002, "Unsteady Effects on the Flow Across Tilting Disk Valves", J. of Bio. Eng, Vol 124, 21-29.

[15]Huang, Z. J., Merkle, C. L., Abdallah, S., Tarbell, J. M., 1994, ''Numerical Simulation of Unsteady Laminar Flow Through a Tilting Disk Heart Valve: Prediction of Vortex Shedding,'' J. Biomech., 27, No. 4, 391–402.